Analysis of Time-Dependent Deformation of CFRP Considering the Anisotropy of Moisture Diffusion

Yoshihiko Arao [a,*], **Jun Koyanagi** [b], **Hiroshi Hatta** [b] and **Hiroyuki Kawada** [c]

[a] Graduate School of Waseda University, 3-4-1 Okubo, Shinjuku, Tokyo 169-8555, Japan
[b] Japan Aerospace Exploration Agency, Institute of Space and Astronautical Science, 3-1-1, Yoshinodai, Sagamihara, Kanagawa 229-8510, Japan
[c] Department of Mechanical Engineering, Waseda University, 3-4-1 Okubo, Shinjuku, Tokyo 169-8555, Japan

Abstract

The moisture absorption behavior of carbon fiber-reinforced plastic (CFRP) and its effect on dimensional stability were examined. Moisture diffusivity in CFRP was determined by measuring a specimen's weight during the moisture absorption test. Three types of CFRP specimens were prepared: a unidirectionally reinforced laminate, a quasi-isotropic laminate and woven fabric. Each CFRP was processed into two geometries — a thin plate for determination of diffusivity and a rod with a square cross-section for the discussion of two-dimensional diffusion behavior. By solving Fick's law expanded to 3 dimensions, the diffusivities in the three orthogonal directions were obtained and analyzed in terms of the anisotropy of CFRP moisture diffusion. Coefficients of moisture expansion (CMEs) were also obtained from specimen deformation caused by moisture absorption. During moisture absorption, the specimen surfaces showed larger deformation near the edges due to the distribution of moisture contents. This deformation was reasonably predicted by the finite element analysis using experimentally determined diffusivities and CMEs. For unidirectional CFRP, the effect of the fiber alignment on CME was analyzed by micromechanical finite element analysis (FEA) and discussed.
© Koninklijke Brill NV, Leiden, 2008

Keywords
CFRP, water diffusion, dimensional stability, fiber alignment

1. Introduction

Carbon fiber-reinforced plastics (CFRPs) are now applied extensively in industrial fields, due to their high specific strength and modulus. The important characteristics of CFRP are its low thermal expansion and excellent dimensional stability. Recently, the demand to assure long-term dimensional stability is growing with

* To whom correspondence should be addressed. E-mail: y.arao@asagi.waseda.jp
Edited by the JSCM

progress in precision engineering and instrument engineering. For instance, the deformation of antenna reflectors must be controlled within a few microns to protect from loss of signal. In such fields, the potential use of CFRP in accurate structures is highly promising. Carbon fibers, with their negative thermal expansion, may make zero-thermal-expansion products possible [1]. However, CFRP has a polymer as its matrix, so it is well known that time-dependent deformations such as the deformation caused by moisture absorption, creep, thermal stress relaxation and polymer shrinkage can occur [2]. The expansion caused by moisture absorption is especially large, so that swelling can be the problem when we design high-accuracy structures [3].

The diffusion behavior into FRP was investigated by Shen and Springer [4]. They obtained the moisture content M and diffusivities D by monitoring the weight change of FRPs. The moisture concentration in the material can be calculated using the equation based on Fick's law. In regard to the diffusivities, Loos and Springer investigated the temperature dependence on the moisture diffusion, and confirmed that these variables are subject to the Arrhenius Law [5]. Water diffusion into a polymer is very slow, and it takes a long time to achieve the saturated condition. So CFRP is usually in the unsaturated state for moisture absorption, and internal stress arises due to the distribution of moisture contents [6–8]. Many researchers have studied the internal stress by numerical analysis, but their researches lack experimental demonstration. On the other hand, moisture-induced strains can be organized by the Coefficient of Moisture Expansion (CME), which is the value normalized by the moisture content M. Collings and Stone obtained CME by measuring the curvature of an asymmetric strip with moisture [9]. In this method, the distribution of the moisture content was not considered, and the expansion in the fiber direction was neglected. Thus, an exact CME could not be obtained with the above method.

The aims of the present research are to investigate the distribution of displacement of materials that have a distribution of moisture content, and to reproduce the deformation caused by moisture absorption with numerical analysis considering the anisotropy of moisture diffusion and CME. The weight changes of CFRPs were monitored to obtain the diffusivities in the three orthogonal directions derived by Fick's law. The displacement of the material in the unsaturated condition was also measured by a three-dimensional measuring system. Then, numerical analysis considering the anisotropy of diffusion was performed with CME as a parameter. The analytical results were compared with the experimental results, and the validity of the numerical analysis discussed. Finally, the effect of fiber alignment against CME was investigated using FEM analysis.

2. Experimental

2.1. Moisture Absorption Test

A moisture absorption test was conducted with a temperature–humidity controlled bath at 80°C, 90% RH. We used two geometries of specimens as shown in Fig. 1 in
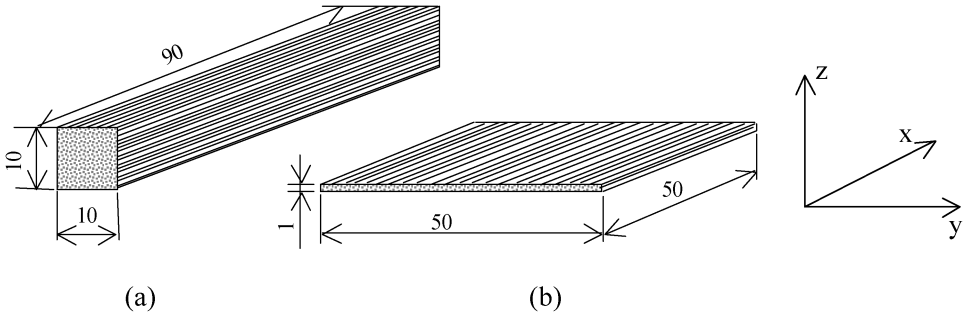
Figure 1. Specimen geometry. (a) rod (UD 0°); (b) thin plate (UD).

the moisture absorption test. Figure 1(a) is the rod specimen ($180 \times 10 \times 10$ mm) with a square cross-section. It was used for measuring dimensional change and weight change. Figure 1(b) is the specimen used for calculating the diffusivity with rod specimens. The other specimens were designed as thin plates ($50 \times 50 \times 1$ mm), which are easy to saturate at an early stage. The specimens used in this study were a unidirectional laminate (0°, 90°), a quasi-isotropic laminate (K13710/AY33, Mitubishi Chemical), and woven fabric (T300/#2500, Toray). Specimens were dried out at 100°C for 72 h with a vacuum oven. Then the specimens were exposed to 80°C, 90% RH with a temperature–humidity controlled bath. After a constant time passed, the weights of specimens were measured by a high-accuracy electronic balance. The moisture absorption rate $M\%$ was defined by the following equation:

$$M = \frac{(W - W_{\mathrm{d}})}{W_{\mathrm{d}}} \times 100, \qquad (1)$$

where W_{d} is the weight of the specimen before moisture absorption, and W is the weight of specimen after absorbing water.

2.2. Measuring the Size of Specimens

After measuring the weight, the rod specimens were attached to a three-dimensional measuring system, and the temperature of the specimens was stabilized at 20°C for an hour. The three-dimensional measuring system was composed of an x–y stage with 1 µm accuracy and a laser finder measuring z-displacement with 0.1 µm accuracy. A schematic diagram of the method for measuring displacement is shown in Fig. 2. The expansion of the long side of the specimen was recorded by the value of the x–y stage, and the laser finder measured the deformation in the thickness direction. CME β is derived by the following equation:

$$\beta = \frac{\varepsilon^{\mathrm{M}}}{M}, \qquad (2)$$

where ε^{M} is the moisture-induced strain. In regard to the CME in the fiber axial direction, it is difficult to obtain the value with our systems, so we adopted Schapery's thermal expansion equation to calculate the CME in the fiber direction [10]. The
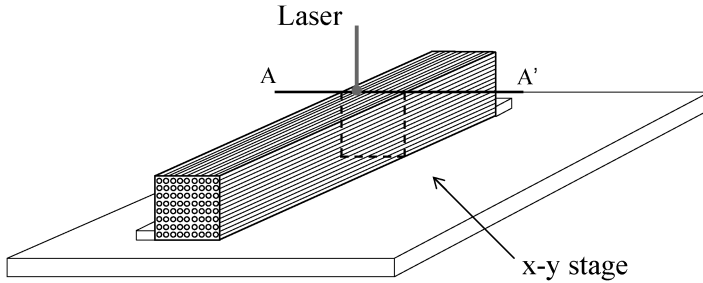
Figure 2. Explanatory diagram for measurements of displacement in the thickness direction.

CME of the fiber is assumed to be 0. We used the following equation to obtain CME in the fiber direction:

$$\beta_T = \beta_m V_m (1 + \nu_m), \tag{3}$$

$$\beta_L = \frac{E_m V_m \beta_m}{E_m V_m + E_f V_f}, \tag{4}$$

where β_m is the CME of the matrix, β_T is the CME of CFRP in the direction perpendicular to the fiber, and β_L is the CME in the fiber axial direction.

3. Diffusivities

3.1. Theory

It has been reported that the diffusion behavior in CFRP follows Fick's law. The second Fick's law is described as follows:

$$\frac{\partial c}{\partial t} = D_x \frac{\partial^2 c}{\partial x^2}, \tag{5}$$

where D_x is the diffusivity in the x direction, and c represents the moisture concentration.

The following approximate equation is obtained to solve equation (5) with the boundary conditions $c = 0$ inside of the model ($t = 0$) and $c = c_m$ on the surface of the model ($t > 0$) [3]:

$$\frac{M}{M_m} = \frac{4}{L\sqrt{\pi}}\sqrt{D_x t}, \tag{6}$$

where M_m is the maximum moisture content. Equation (6) shows that M varies linearly with the square root of time, and is accurate when $\sqrt{Dt}/L$ is very small, in other words, in the early stage of the moisture absorption test. In the early stages of the process, equation (6) might be applied to each side independently, and expanded as follows:

$$M = 4M_m \left(\frac{1}{l}\sqrt{D_x} + \frac{1}{w}\sqrt{D_y} + \frac{1}{h}\sqrt{D_z} \right)\sqrt{\frac{t}{\pi}}. \tag{7}$$

The independent coefficients D_x, D_y, D_z. X, y, z represent the directions shown in Fig. 1, respectively. In the case of quasi-isotropic laminate and woven fabric, D_x and D_y, which are the diffusivities of the in-plane direction, would be equal. So we can obtain D_x and D_z when the weight change is monitored for two types of specimens as shown in Fig. 1(a) and 1(b), and of equation (7) is solved simultaneously. We assumed that there are three independent parameters in the unidirectional laminate, and calculated the diffusivities in the three orthogonal directions.

3.2. Result of Moisture Absorption Test

Figure 3 shows the moisture content against the square root of time. Figure 3(a) is the result of the thin plate specimen. All thin plate specimens were saturated after 400 h. Figure 3(b) is the result of the rod specimens. The rod specimens were still not saturated after 1 month due to their thickness. Moisture contents are in proportion to the square root of time below 1% of moisture content, so it is obvious that equation (7) is available at the initial stage of the test.

The diffusivity in each direction was calculated with equation (7) and the initial slope of the test results shown in Fig. 3. There are three unknown parameters in equation (7). So in the case of unidirectional laminates, we calculated the simultaneous equation of the results of three different shapes of specimens. In regard to the quasi-isotropic laminates and woven fabrics, we assumed the unknown parameters were the two parameters of the thickness direction and the in-plane direction. Their diffusivities were obtained from the results of thin plate specimens and rod specimens. Table 1 shows the diffusivities for all specimens. D_x and D_y are in-plane directions; D_x is the diffusivity of the fiber axial direction and D_y is the diffusivity of the in-plane transverse direction. D_z represents the diffusivity of the thickness direction. From the results, D_x was 2–4 times greater than that of other directions. If the fibers were assumed to act as a barrier to penetrating water molecules, the water molecules would make a detour around the fibers, and the diffusion route gets longer when the water molecules diffuse in the transverse direction. Therefore D_x, which is the diffusivity of water molecules in the fiber axial direction, might be greater than the other values [11]. In addition, D_y was two times greater than D_z though both D_y and D_z represent the transverse direction in a unidirectional laminate. It is presumed that the distance between each fiber might be different between the thickness direction and in-plane direction; more specifically the length of the diffusion route is different between them. Comparing D_z of the unidirectional laminate and quasi-isotropic laminate, it was observed that the diffusivities are not influenced by the stacking sequence.

4. Dimensional Change due to Moisture Absorption

4.1. Result of Measuring Displacement

Figure 4 shows the distribution of displacement of rod specimens in the thickness direction with time obtained by a laser finder. The lines drawn in Fig. 4 are the re-
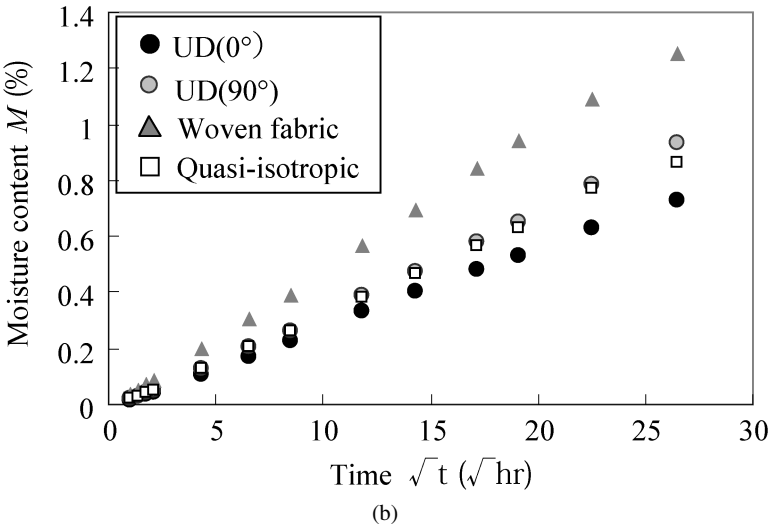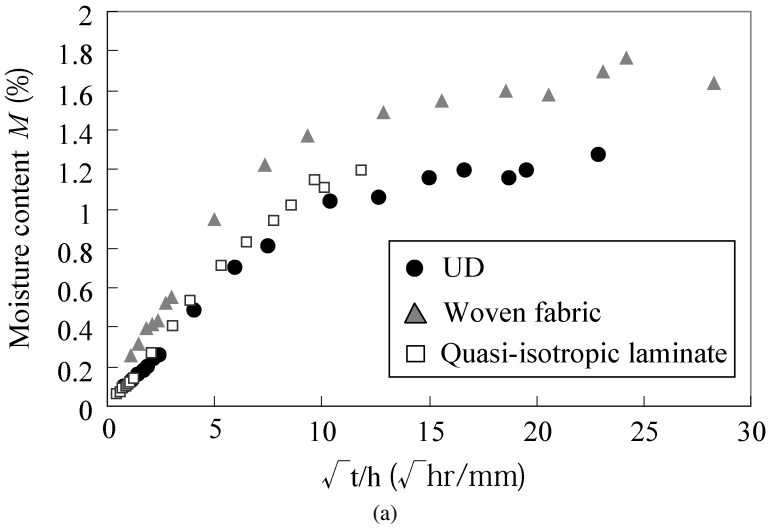
Figure 3. Variation of moisture content of CFRP composite with the square root of exposition time in moisture environment. (a) Moisture uptake for thin plates; (b) moisture uptake for rods.

Table 1.
Comparison of diffusivities

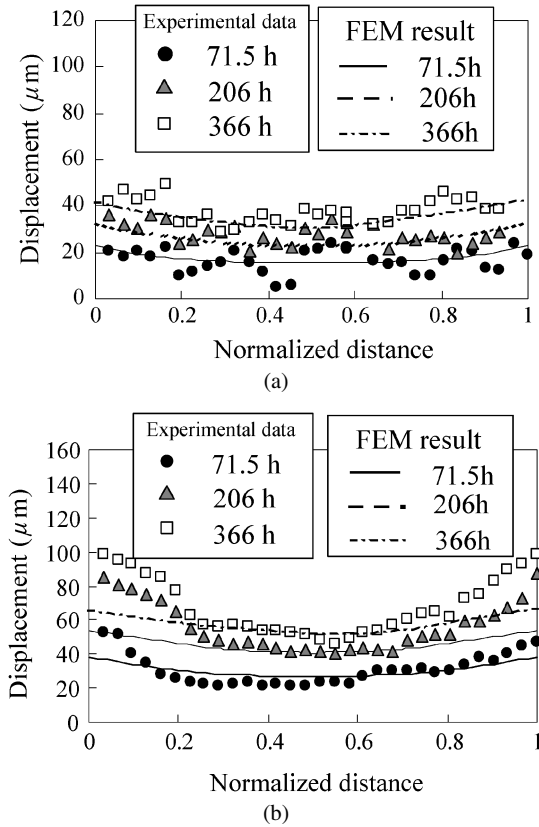| Material	Diffusivities D_x (mm²/h)	Diffusivities D_y (mm²/h)	Diffusivities D_z (mm²/h)
UD	0.00555	0.00244	0.00131
Qusasi-isotropic laminate	0.00459	0.00459	0.00133
Woven fabric	0.00482	0.00482	0.00227

Figure 4. Distribution of displacements of the various composites in the thickness directions due to the water diffusion. (a) UD (0°); (b) UD (90°); (c) woven fabric; (d) quasi-isotropic laminate.

sults of finite element analysis (FEA), discussed later. The horizontal axis in Fig. 4 shows the normalized values (y/B) of width ($B = 10$ mm), and the vertical axis shows the absolute value of dimensional change due to moisture absorption. It was observed that the corner of the specimens swelled more than other positions. This result is explained by the fact that the moisture concentration is greater near the surface of specimens in the unsaturated state. The deformation and curvature of the specimen's surface on 90° UD (90 degree unidirectional laminates) were larger than that of 0° UD (0 degree unidirectional laminates). This is due to the fact that the diffusion in the width direction is fast in the 90° UD, and the moisture concentration near the edge is greater than that of 0° UD. The woven fabric showed the largest curvature for all kinds of specimens. This is due to the fact that the maximum moisture content of woven fabric is greater than that of other materials as shown in Fig. 3 and the moisture content is highest near the edge.

4.2. Determination of CME Using FEA

From the above experimental results, FEA analysis was conducted to obtain precise CMEs. It has been known that moisture diffusion is analogous to thermo-diffusion
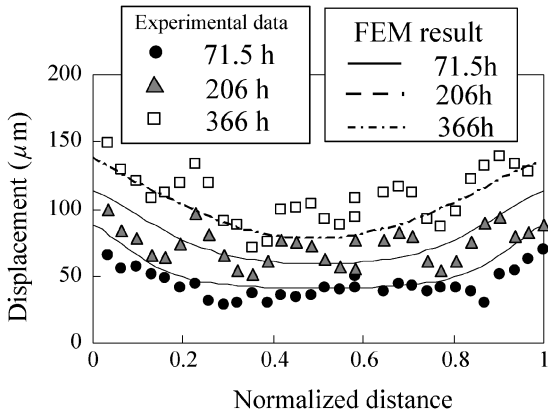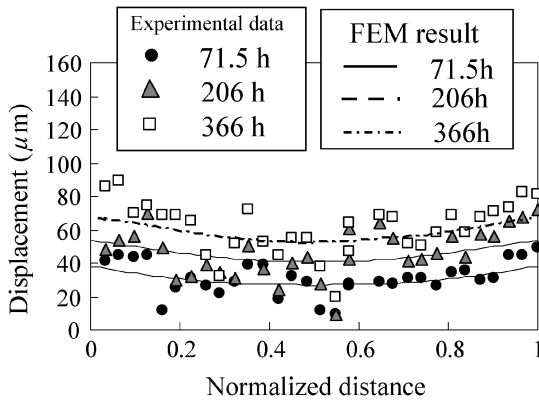
Figure 4. (Continued.)

[12], so the moisture absorption was calculated using the elements of thermal conduction. The diffusivities used in this analysis are listed in Table 1. FEA considering the anisotropy of water diffusion was conducted. Figure 5 shows the FEA model. The model was simplified to 2 dimensions, representing the cross-section of the rod specimens. The boundary conditions applied in this analysis are as follow:

(1) The y-displacement ($v = 0$) was constrained on nodes of $(y, z) = (0, 0)$ and $(y, z) = (0, 10)$. Additionally the z-displacement ($w = 0$) was constrained on nodes of $(y, z) = (0, 0)$ and $(y, z) = (10, 0)$.

(2) The maximum moisture content M_m was given on all nodes of the boundary. M_m was obtained from the saturated values shown in Fig. 3; $M_m = 1.3\%$ for unidirectional and quasi-isotropic laminates and $M_m = 1.7\%$ for woven fabric.

The elements used in this analysis were quadrate thermal conduction elements and plane strain elements. The material properties obtained from the static test are
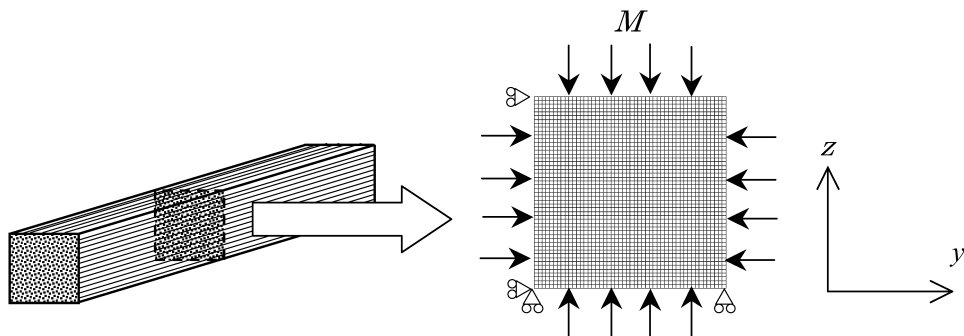
Figure 5. FEA model.

Table 2.
Material properties

	E_y (GPa)	E_z (GPa)	ν_{yz}	G_{yz} (GPa)
UD (0°)	5	5	0.3	4
UD (90°)	350	5	0.3	4
Woven fabric	54	5	0.3	4
Quasi-istoropic laminate	130	5	0.3	4

shown in Table 2. One-directional coupling analysis was conducted. In this analysis, the thermo-diffusion is calculated first; then the stress analysis is performed with CME as a parameter. The CMEs in the thickness direction are the fitting parameters.

Figure 4 shows a comparison between the experimental results and analytical results. The analytical results show good agreement with the experimental results, except for the result of 90° UD. In regard to the 90° UD quasi-isotropic laminates, the swelling at the edge is larger than that of analytical results. It is presumed that the shear stress relaxation of the fiber/matrix interface at the edge might be affected. Compression stress arises in the fiber and tensile stress in the matrix during molding due to the thermal mismatch between the matrix and the fibers. So, interfacial shear stress is generated at the edge of specimens. Viscoelastic deformation arises when this interfacial shear stress is released over time. This time-dependent behavior could affect the displacement in the thickness direction. The curvature of the specimen's surface is different between experimental results and analytical results in the 90° UD, so we determined CME to fit the data except for the data at the edge. The CME obtained from 90° UD corresponded to the CME obtained from 0° UD, and is shown in Table 3. From Table 3, the CME of the thickness direction is about two times larger than the CME of the in-plane transverse direction, despite the fact that both directions are perpendicular to the fiber axis. This CME's difference has been confirmed in other researches, and the CME differs by about 2–3 times [2, 11].

Table 3.
Coefficient of moisture expansion

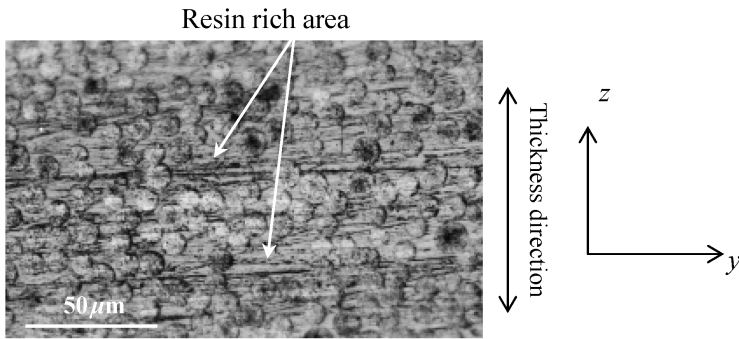| Material	Direction	CME (/%)
Unidirectional laminate	$\beta_{0°}$	0.32×10^{-4}
	$\beta_{90°}$	33×10^{-4}
	$\beta_{\text{thickness}}$	67×10^{-4}
Woven fabric	$\beta_{0°}$	2.1×10^{-4}
	$\beta_{\text{thickness}}$	110×10^{-4}

Figure 6. Cross-sectional photograph of unidirectional laminate.

5. Discussion

As shown in Table 3, the CME of the thickness direction is different from the CME of the in-plane transverse direction. The voids exiting at the interlaminates might affect the difference of CME [11], but no voids or interlaminates were observed in these specimens, as shown in Fig. 6. The specimens used in this study were fabricated from prepreg tape using an autoclave. So the fibers would be dense in the in-plane direction, and resin-rich areas were observed, as shown in Fig. 6. The density of fiber distribution could be different between the thickness direction and in-plane transverse direction. That is, if only the matrix is assumed to swell, it is expected that the expansion in the in-plane direction could be small and the expansion in the thickness direction could be large. Therefore we considered that the fiber alignment caused the difference of CME in the transverse directions. In the following section, we focus on the fiber alignment and discuss the effect of the fiber distribution on CME.

Micromechanical FEA was performed to obtain CMEs in various fiber alignment with the same V_f. The fiber alignments are assumed to be the lozenged alignments, as shown in Fig. 7(a). The alignment shown in Fig. 7(b) is dense in the in-plane direction (y-direction). To obtain the CME of CFRP with this fiber alignment, we considered the unit cell model shown in Fig. 7(c). In this analysis, only the matrix

swells with absorbed water, and the CME of the thickness direction and in-plane direction are calculated analytically. In Fig. 7(c), a and b are associated with the following equation:

$$(a + r)(b + r)V_f = \frac{\pi r^2}{2}. \tag{8}$$

In the above equation, V_f is a constant value ($V_f = 0.5$). If r is assumed to be 1, a can be determined with b, which is given arbitrarily. In the case of square alignment, a and b are the same value. We develop the discussion with k, which is the aspect ratio of the unit cell model, or the coefficient that indicates the deviation of the fiber distribution. When $k = 1$, the distance between fibers in the thickness direction is equal to that of the in-plane direction, and the CMEs are equal in both directions:

$$k = \frac{r + a}{r + b}. \tag{9}$$

Figure 8 shows the 2-dimensional finite element model used in this study. The symmetric condition was applied to the boundary of $y = 0$ and $x = 0$. The degrees
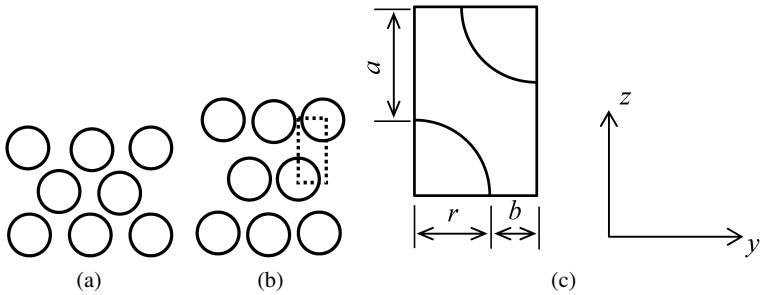

Figure 7. Fiber distribution model. (a) Lozenge alignment; (b) including resin rich model; (c) least unit.
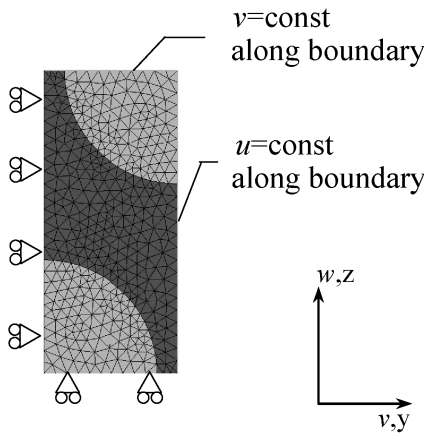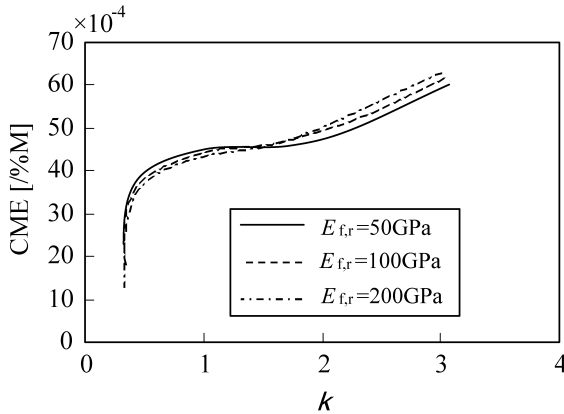

Figure 8. FEA model.

Figure 9. CME with various fiber alignments.

of freedom on the nodes of the other boundary were imposed considering the periodicity. The CMEs are $\beta_{\rm m} = 80 \times 10^{-4}/\%$ for the matrix, and $\beta_{\rm f} = 0/\%$ for the fibers. The CME of CFRP was obtained from the equation below:

$$\beta = \frac{\Delta l}{l_0} \frac{1}{\Delta M},$$

where l_0 is the former length and Δl is the dimensional change by moisture absorption. The elastic modulus of the matrix was 5 GPa, and the elastic modulus of the fibers in the radial direction was measured using the parameters of 50, 100, 200 GPa. Figure 9 shows the analytical results of CMEs. The vertical axis is the CME, and the horizontal axis is k, i.e. the aspect ratio of the unit cell. The CME gets smaller at $k = 1$ with an increase the elastic modulus of fibers due to the increase of apparent modulus of the unit cell. In the range of this analysis, no large differences of CME were observed with the difference of fiber modulus. The difference of CMEs by fiber alignment was largest when the elastic modulus of fibers was 200 GPa. CME varied exponentially when k was below 0.5 or above 2.0. The least value was $15.8 \times 10^{-4}/\%$M, and maximum value was $62.7 \times 10^{-4}/\%$M. Hence, the maximum difference of CME between the thickness direction and the in-plane direction is about 4 times.

To obtain the k value of the specimens used in this study, the following evaluation of fiber distribution was conducted based on the photograph of Fig. 6. Square areas including about 20 fibers were extracted from Fig. 6. We decided the center of the square area as the origin of coordinates and found the coordinates of all fibers of the center in the square area. When v and w are defined as the components of the coordinate of center of the fibers in the thickness direction and the in-plane direction respectively, k could be evaluated by the following equation:

$$k = \sum_{n=1}^{n} w_n \Bigg/ \sum_{n=1}^{n} v_n. \tag{10}$$

Values of k were obtained for 10 arbitrary areas. The average value of k was 1.5. The CMEs of $k = 1.5$ were $45.8 \times 10^{-4}/\%M$ for the thickness direction and $41.6 \times 10^{-4}/\%M$ for in-plane direction, and the difference in CME between the thickness direction and the in-plane direction was about 10%. We confirmed that the CMEs vary with the fiber alignment. Though $k = 1.7$, the rate of CME for thickness and in-plane direction is 1.3, and this value comes short of the experimental value of 2.0. It was concluded that the fiber alignment affects the difference of CMEs for the thickness direction and in-plane direction, but other factors such as the anisotropy of the matrix contribute.

On the other hand, the fiber alignment might affect the difference in diffusivities for the thickness and in-plane transverse directions shown in Table 1, because the value of k is connected to the diffusion route. More specifically, in the case of the alignment shown in Fig. 7(b), it can be explained qualitatively that the diffusivity of the in-plane direction D_y is larger than the diffusivity of thickness direction D_z because the route of diffusion in the in-plane direction is wider.

Furthermore, the ratio of CMEs for the thickness direction and in-plane direction is about 2 while the ratio of diffusivity for the thickness direction and the in-plane direction is about 0.5. This is consistent with the fact that both rates are generated from the same factors. There might be some correlation between CMEs and diffusivities. Discovering the mechanism which generates the difference of CME or diffusivity is a challenge for the future.

6. Conclusion

The diffusivities in the three orthogonal directions were obtained by solving a simultaneous equation, which was given by a moisture absorption test with two shapes of specimens. Generally, the diffusion in the direction of the fiber axis is speedy, about 2–4 times larger than those of other directions. From the results of measuring the displacements at various unsaturated states, it was confirmed that the displacements at the positions with high moisture contents were larger than those of other positions.

Coupling analysis, which included diffusion analysis and stress analysis, was performed, and compared to the experimental results. FEA was conducted with CME as a parameter, and CMEs were obtained with consideration of the distribution of moisture contents. The analytical results showed good agreement with the experimental data for all times. The CME in the thickness direction was two times larger than that in the in-plane transverse direction. The CME of CFRP in transverse direction was analyzed by using a micromechanical model considering the fiber alignment. The fiber alignment affects the difference of CME in the thickness direction and the in-plane transverse direction, but other factors are also considered to affect this behavior.

Acknowledgements

References

1. A. Kelly, R. J. Stearn and L. N. McCartney, Composite materials of controlled thermal expansion, *Compos. Sci. Technol.* **66**, 154–159 (2006).
2. E. G. Wolff, *Introduction to the Dimensional Stability of Composite Materials*, DEStech Publications, Lancaster, PA (2004).
3. T. Ozaki, K. Naito, I. Mikami and H. Yamauchi, High precision pipes for SORAR-B optical structures, *Acta Astronautica* **4**, 85–120 (2001).
4. C. H. Shen and G. S. Springer, Moisture absorption and desorption of composite materials, *J. Compos. Mater.* **10**, 2–21 (1976).
5. A. C. Loos and G. S. Springer, Moisture absorption of graphite/epoxy composites immersed in liquid and in humid air, *J. Compos. Mater.* **13**, 131–147 (1979).
6. A. Benkeddad, M. Grediac and A. Vautrin, Computation of transient hygroscopic stresses in laminated composite plates, *Compos. Sci. Technol.* **56**, 869–876 (1996).
7. A. Benkeddad, M. Grediac and A. Vautrin, On the transient hygroscopic stresses in laminated composite plates, *Compos. Struct.* **30**, 201–215 (1995).
8. A. Tounsi and E. A. Adda Bedia, Some observations on the evaluation of transversal hygroscopic stresses in laminates composites plates: effect of anisotropy, *Compos. Struct.* **59**, 445–454 (2003).
9. A. Collings and D. E. W. Stone, Hygrothermal effects in CFRP laminates: strains induced by temperature and moisture, *Composites* **16**, 307–316 (1985).
10. R. A. Shapery, Thermal expansion coefficients of composite materials based on energy principles, *J. Compos. Mater.* **2**, 380–404 (1968).
11. H. S. Choi, K. J. Ahn and J. D. Nam, Hygroscopic aspects of epoxy/carbon fiber composite laminates on aircraft environment, *Composites, Part A* **32**, 709–720 (2001).
12. D. F. Adam and F. Donald, Hygrothermal microstresses in unidirectional composite exhibiting inelastic material behaviour, *J. Compos. Mater.* **11**, 285–299 (1977).